



www.editada.org

Planar antenna design for contactless energizing applications: resonance analysis

Jorge Santiago-Amaya^{1†}, Diego Escamilla-Amador¹, Francisco R. Trejo-Macotela² and Daniel Robles-Camarillo^{2‡}

¹Technological of Higher Studies of Chalco (TESCHA), Mexico.

²Polytechnic University of Pachuca (UPP), Mexico.

^{1†}jorge_sa@tesch.edu.mx

^{2‡}danielrc@upp.edu.mx

Abstract. Advances in medical technology suggest that the application of implantable medical devices or Smart Hospital Devices (SHD) can enhance the control and treatment of chronic disorders. However, most of these developments require an electrical power source for operation, making the use of batteries unfeasible. This paper presents the design and resonance analysis of four different geometries for the fabrication of planar antennas as an alternative to a contactless power supply. Previously published software (Santiago-Amaya, López-García, Aguilar-Guggembuhl, Sánchez-Díaz, 2022) was used to calculate the electrical parameters for each coil design. Operating trials were executed under laboratory conditions, and a bracket manufactured using polylactic acid (PLA) through a 3D printer was used to accurately define the distances between coils to achieve correct alignment between them. Based on the experimental results, it was possible to calculate the resonant frequency of the inductive links at a 5 mm spacing. Similarly, it is possible to calculate the capacitive effect necessary to improve the resonant circuit in different transmitter-receiver planar antenna pairs. The most efficient combination to induce voltage in these links is to use the hexagonal profile design as a transmitter and receiver antenna, applying a sinusoidal signal with 8 MHz frequency.

Article Info

Received Sep 27, 2023

Accepted Dec 12, 2023

1 Introduction

The efficiency of inductive links has been under investigation in recent decades, for use in different applications, from cards and smartphones to wearable smart hospital devices (SHD) that can be implanted in an organism. This issue has considerable limitations and is due to the morphological characteristics of each living being (Fang, Hou, Zhou & Zhang, 2018). A particular case is the monitoring of ventricular pressure with a maximum dimension of 1.8 cm² as mentioned by (Hernández-Sebastián, Renero-Carrillo, Díaz-Alonso & Calleja-Arriaga, 2019). The importance of a study to energize a medical device small enough is relevant, to treat degenerative diseases, such as diabetes, arterial hypertension, cancer, eye diseases, or other pathologies that must always be controlled by the patient. There are devices that can be energized with batteries and implanted in an organism; however, this method is not viable owing to the size and lifetime of the batteries and their energization. The alternative considered in most studies focuses on inductive links using planar antennas (Abbas, Hannan, Samad, & Hussain, 2014).

The objective of this study is to find the most appropriate way to measure the absorption of a flat receiver coil, which is intended to determine the appropriate geometry for wireless transmission between two coils. The first studies focused on wirelessly measuring the pressure of the eyeball (Hernández-Sebastián et al, 2019; Hernández, 2020; Rendon-Nava et al., 2014) through an impedance bridge in the transmitting coil, whereas Rendon-Nava et al. (2014) proposed a variable capacitor inserted in the anterior chamber of the eyeball and connected in series to the receiving coil to measure of intraocular pressure. Natiely describes the propagation of magnetic fields of circular flat coils for inductive power transfer (IPT) in tissues whose proposed working frequency is 13.56 Mhz with a separation of 3.5 cm, another relevant study was performed by Ongayo, et al. (2015), in this study proposes an aluminum foil behind the coils to contain the inductive link. Various studies have demonstrated the propagation of magnetic fields using simulation software. However, there are still no clear experimental studies on the response

of inductive links to different geometries. In the present work, we intend to establish a clear idea of the frequency response of the square, circular, hexagonal, and octagonal coils.

1.1 Organization

This paper is organized as follows. In section two, it's shown a documentary review of the main works that propose a fundamental analysis for the design of planar antennas and their respective parameters is presented. Section three presents the methodology developed to physically experiment with the different designs developed in this research and discusses in detail the applied measurement process. Section four presents the results obtained for trials using the designed planar antennas to identify the necessary characteristics and parameters that improve the resonance of the inductive links. Finally, we conclude by analyzing the most important details identified in the results.

2 Background

Different geometries were used for the wireless power transmission. Zhao et al. (2010), proposed a mathematical expression defining the inductance of four different planar geometries, as given in (1).

$$L = \left[\frac{(\mu_0 N^2 D_{avg} C_1)}{2} \right] \left[\ln \left(\frac{C_2}{\rho} \right) + C_3 \rho + C_4 \rho^2 \right] \tag{1}$$

where ρ is equal to the filling ratio; D_{avg} is the average of the inner A, C, and outer B and D diameters in Figure 1; L is the coil inductance; μ_0 is the space permeability; and the constants C_1 , C_2 , C_3 , and C_4 are determined by the geometries of each coil, as shown in Table 1.

Table 1. Coefficients for inductance of different antennas' geometries [27]

	C_1	C_2	C_3	C_4
Square	1.27	2.07	0.18	0.13
Hexagonal	1.09	2.23	0	0.17
Octagonal	1.07	2.29	0	0.19
Circular	1	2.46	0	0.2

Harrison et al. (2007) defines the mutual inductance of inductive links of perfectly aligned flat coils in parallel each other, as shown in Figure 1. Equation 2 shows the mathematical expression for this phenomenon.

$$M = \frac{1}{2} \mu_0 \sqrt{d_T d_R} \left[\left(\frac{2}{f} - f \right) K(f) - \frac{2}{f} E(f) \right] \tag{2}$$

Where M is the mutual inductance and $K(f)$ and $E(f)$ represent the full elliptic integrals, which can be represented by Taylor's series, as shown in Equations 3 and 4.

$$K(f) = \frac{\pi}{2} \left[1 + \left(\frac{1}{2} \right)^2 f^2 + \left(\frac{1 \cdot 3}{2 \cdot 4} \right)^2 f^4 + \left(\frac{1 \cdot 3 \cdot 5}{2 \cdot 4 \cdot 6} \right)^2 f^6 + \dots \right] \tag{3}$$

$$E(f) = \frac{\pi}{2} \left[1 - \left(\frac{1}{2} \right)^2 f^2 - \left(\frac{1 \cdot 3}{2 \cdot 4} \right)^2 \frac{f^4}{3} - \dots - \left(\frac{(2n-1)!!}{(2n)!!} \right)^2 \frac{f^{2n}}{2n-1} - \dots \right] \tag{4}$$

d_R and d_T are the receiver and transmitter diameters, respectively, and f is a function that depends on the displacement z and the diameter of each coil, which is determined in (3).

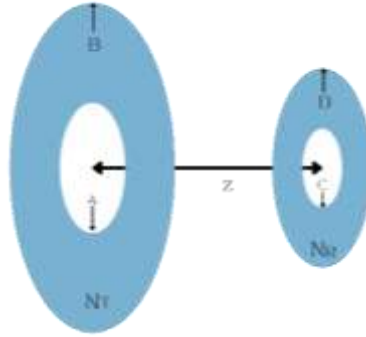


Fig. 1. Flat coil coupling, N_T and N_R represent the number of turns in each planar antenna.

$$f(d_T, d_R, z) \equiv \sqrt{\frac{4d_T d_R}{(d_T + d_R)^2 + z^2}} \tag{5}$$

Each M obtained over the combinations of circles A, B, C and D is averaged to obtain the total M , as shown in (4).

$$M \approx N_T N_R \left[\frac{M_{AC} + M_{AD} + M_{BC} + M_{BD}}{4} \right] \tag{6}$$

A factor to consider when designing planar antennas is the misalignment of the inductors, which decreases the link efficiency. Abbas et al. (2014) establishes these cases considering four in specific, as shown in Figure 2.

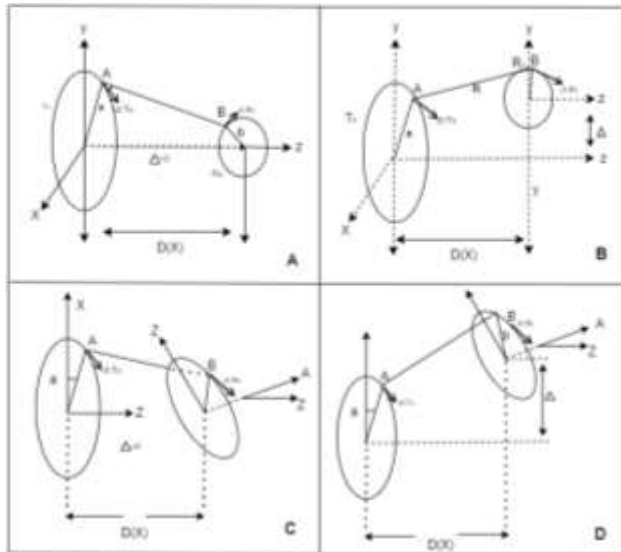


Fig. 2. Cases in which flat coils can be decoupled: A) perfect alignment. B) Lateral misalignment. C) Angular misalignment. D) General misalignment (Abbas, Hannan, Samad, & Hussain, 2014).

In the first case, both coils were perfectly aligned (Figure 2 A). In the second case, they were laterally misaligned (Figure 2 B). In the third case, the coils were out of alignment with respect to their angles (Figure 2 C). Finally, in case four, the coils were laterally misaligned and uncoupled with respect to their angles. For these cases, Abbas et al. used (5) to describe the maximum

or minimum mutual inductance M^* of the bond.

$$M^* = \mu_0 \sqrt{ab} * G(F^*) \quad (7)$$

Where a and b are the radii of the transmitting and receiving coils, respectively, and $G(F^*)$ is a proportion function according to the radius of each coil and their misalignment, which is defined by (6).

$$G(f) = \left(\frac{2}{f} - F^* \right) K(f) - \frac{2}{f} E(F^*) \quad (8)$$

In (5) M^* represents M_{min} or M_{max} and corresponds to F^* equal to F_{min} or F_{max} as appropriate, where F^* represents the misalignment of the coils. This definition is shown in (7). Δ is equal to the misalignment and d equals the distance between the coils. In (5), M^* represents M_{min} or M_{max} and corresponds to F^* equal to F_{min} or F_{max} , as appropriate, where F^* represents the misalignment of the coils. This definition is shown in (7). Δ is equal to the misalignment and d is the distance between the coils.

$$F^* = \sqrt{\frac{4a(b-\Delta)}{(a+b-\Delta)^2 + d}} \quad (9)$$

$$M = \frac{M_{max} + M_{min}}{2} \quad (10)$$

Santiago et al. (2022) use the above equations to code a software to find the electrical characteristics of different planar geometries and performed an analysis of two square flat coils of two different diameters. In the present work, three different tests were performed to determine the most efficient planar antennas' geometries for inductive links.

3 Methodology

The software developed by Santiago et al. (2022) calculates the layout of the geometries and the inductive and resistive parameters of each one of them. The parameters of four geometries (square, octagonal, hexagonal, circular) were calculated. Each of them was created as a single-layer copper PCB coil with 10 turns each, the width and separation of the tracks were one millimeter, the inner diameter was one centimeter, while the outer diameters were approximately five centimeters, depending on the geometry of the coils. The data of the electrical characteristics of these geometries are shown in Table II, the physical flat coils are presented in Figure 3.

Table 2 electrical characteristics of calculated coils, w is the angular frequency for trials.

Geometry	Inductance (μH)	Resistance (Ω)	Quality Factor Q
Square	3.39	1.4	$w * 22.4 * 10^{-6}$
Circular	2.84	1.0	$w * 26.28 * 10^{-6}$
Octagonal	2.76	1.0	$w * 26.59 * 10^{-6}$
Hexagonal	2.72	1.1	$w * 25.77 * 10^{-6}$

Figure 4 shows the block diagram representing the settings used to perform the experiment. The sinusoidal signal is from a UNI-T UTG900 function generator (Yang, Cui, & Cui, 2020), with frequency range from 1 MHz to 60 MHz, and amplitude adjusted to 10 peak-to-peak voltage. The electronic circuit that represents the diagram in Figure 4 is shown in Figure 5 where C_{RNC} is equivalent to 138 pf and r_{bn} has a value of 0.6 ohms, while R_{LTX} and L_{TX} correspond to the inductive values of the transmitting coil, while r_{rx} , R_{LTX} and L_{RX} are equivalent to the values of the transmitter coil that are determined in table 2, in

turn, the readings are received from point a and b in figure 5, by the oscilloscope already specified.

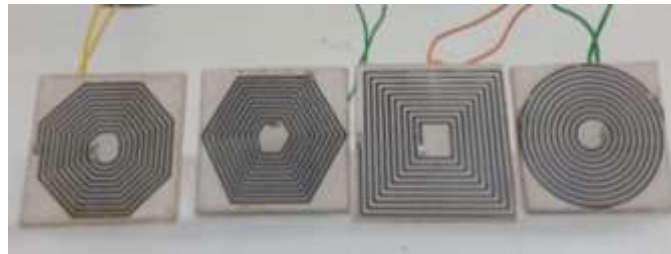


Fig. 3. Four different inductors geometries for inductive link trials.

The measurement of each signal was acquired with the TEKTRONIX TDS 2012C oscilloscope (Montoya, Free, Gunderson, & Preheim, n.d.). In the same way, this device was used to measure the voltage amplitude on the induced signal in the receiving coil.

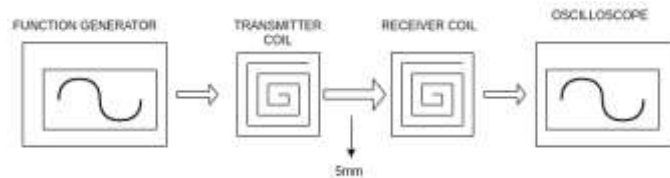


Fig. 4. Block diagram of the elements implemented for physical coil trials.

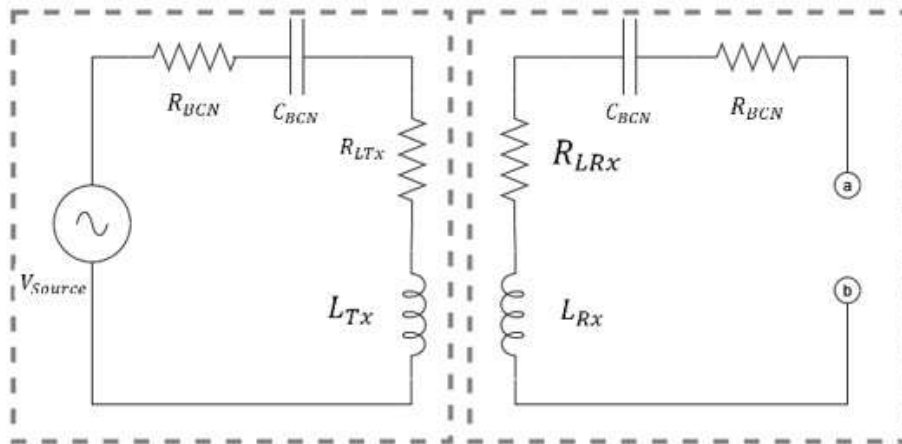


Fig 5. Equivalent circuit of transmitting coil and transmitting coil over the block diagram shown in diagram 4.

To control the alignment and separation between transmitter and receiver antennas, different models of brackets were created with the Pro2 3D Printer (Shi et al., 2014) shown in Figures 5 and 6 where case “A” mentioned by Abbas et al. was used (Abbas, Hannan, Samad, & Hussain, 2014). These parts were designed as supports for each coil and cabinet of the BNC connectors. The tests were performed with a separation distance of 5 mm between coils, keeping them in parallel, and with no tilt angle between them.

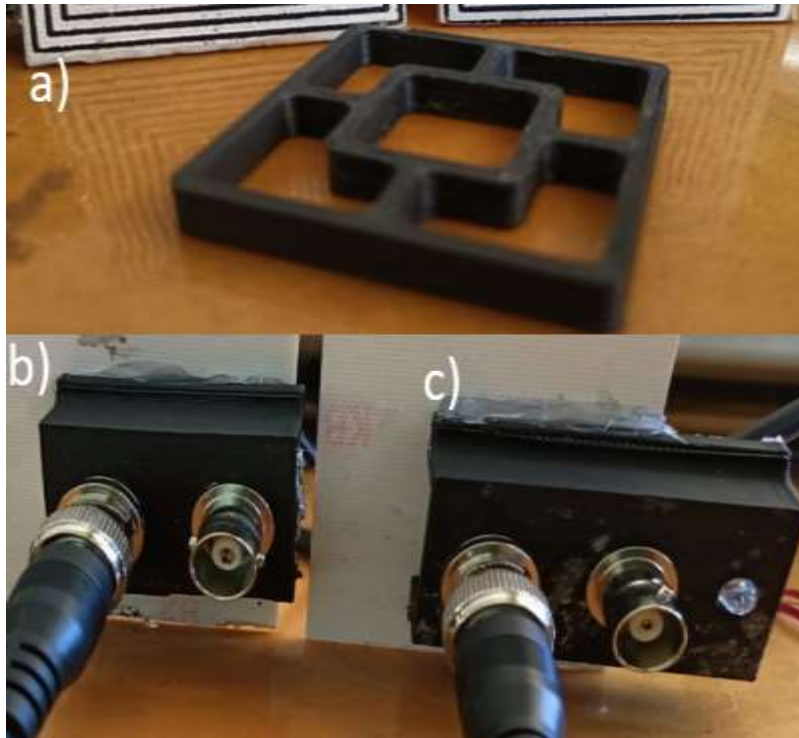


Fig. 6. a) Bracket for the gap between inductors. b) Bracket for transmitter coil and BNC connector. c) Bracket for receiver coil.

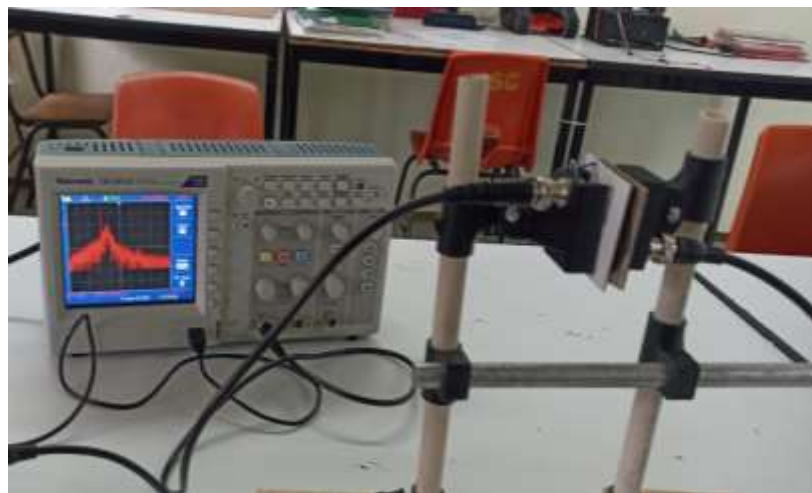


Fig. 7. The tests were performed using different coils with a function generator and an oscilloscope.

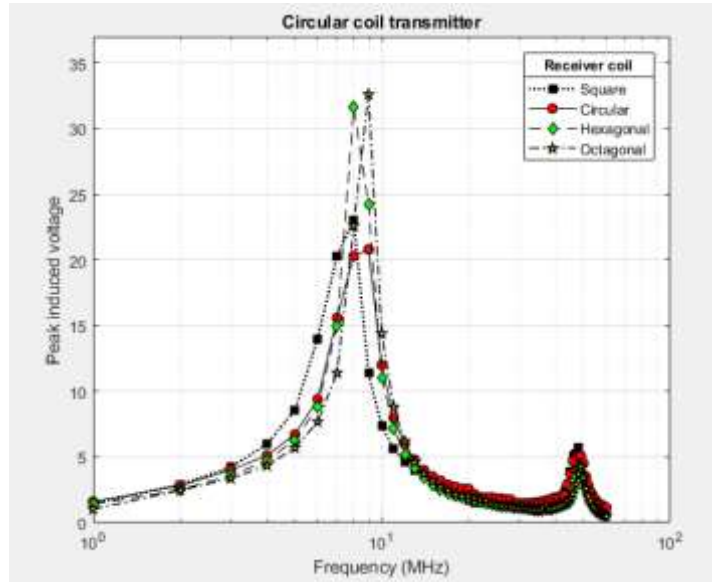


Fig. 8. Measure of induced voltage using the transmitting circular coil

In Fig. 9, the octagonal transmitter can induce up to 28.8 volts at 8 MHz on the square coil as the receiver. The second rush was measured for 7.12 volts at 48 MHz, using an octagonal shape as the receiver antenna.

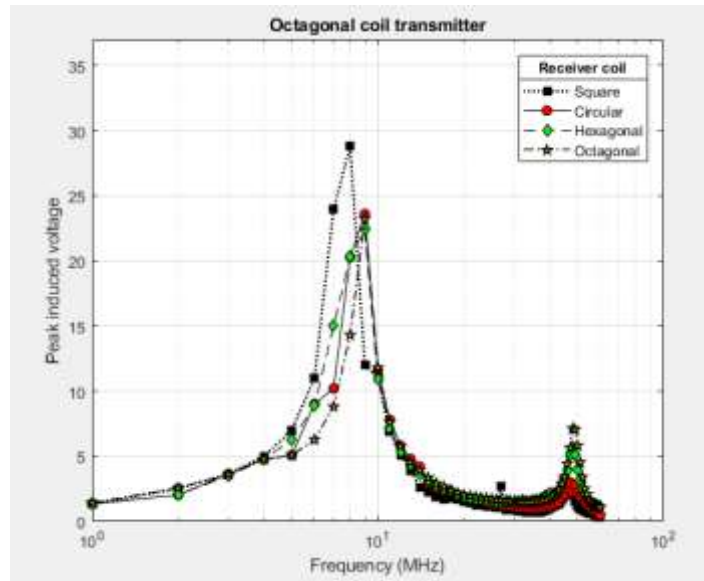


Fig. 9. Measure of induced voltage using the transmitting octagonal coil

The last experiment shown in Fig. 10 was used the hexagonal shape as transmitter antenna and hexagonal coil shape as receiver antenna. The second rush in the same experiment occurred at 48 MHz when it was used the octagonal shape as receiver antenna with 7.12 volts.

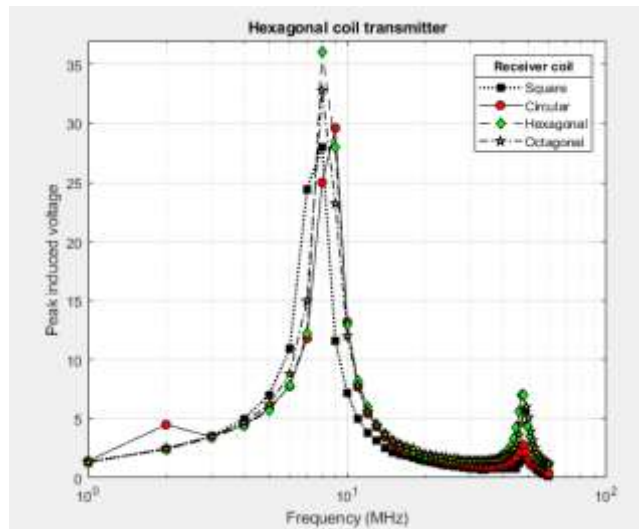


Fig. 10. Measure of induced voltage using the transmitting hexagonal coil

Table 3 lists the maximum induced voltages (Volts) measured in the receiver coil and the frequency applied to the transmitter coil. The most efficient pair is the hexagonal transmitter and receiver. The maximum measured voltage was 32.8 V when the transmitter was set to 8 MHz. On the other hand, when is used the square transmitter and square receiver, the maximum induced voltage is 14.1 V at 7 MHz.

Table 3 Maximum induced voltage per geometry and frequency

Transmitter	Receiver coil geometry			
	Induced voltage (Volts) per frequency (MHz)			
Square	14.1/7	17.6/8	14.7/8	18.0/8
Circular	23.0/8	20.8/9	32.6/9	31.6/8
Octagonal	28.8/8	23.6/9	23.2/9	22.4/9
Hexagonal	28.0/8	29.6/9	30.6/8	32.8/8

In the same experiments, it was possible to measure the second rush of the induced voltage for all combination pairs. Table 4 summarizes the results. When the octagonal transmitter was connected to the 48 MHz source, and the octagonal coil was used as the receiver antenna, the induced voltage was 7.12 V. On the other hand, the same octagonal transmitter, but using a square receiver, induces only 0.842 V at 48 MHz. The origin of this second voltage rush was unclear.

Table 4. Second rush of maximum induced voltage per geometry and frequency

Transmitter	Receiver coil geometry			
	Induced voltage (Volts) per frequency (MHz)			
Square	3.3/47	3.34/48	0.842/48	0.12/48
Circular	5.68/48	5.08/48	3.7/48	4.28/48
Octagonal	2.38/47	3.0/47	7.12/48	5.68/48
Hexagonal	2.0/47	2.78/47	6.0/49	7.04/48

4 Conclusion

The trials performed in this work demonstrate that there is an induced voltage higher in the receiver coil than the voltage applied to the transmitter coil, which is described by Faraday's law. This indicates that the voltage induced by a conductor is determined by several factors such as magnetic permeability, conductors' transversal section, and induced current passing through them (Liu, Xia, Yuan, 2018), among others. In this sense, there is a frequency bandwidth from 6 MHz to 8 MHz, in which the maximum voltage is induced in all receiver coils. Finally, the combination of inductive pairs is determined. The highest gain occurred when the hexagonal shape was used as the receiver and transmitter coil. The best way to transmit energy in planar antennas is applying 8 MHz of frequency to the transmitter coil, both of which have the same hexagonal geometry.

4.1 Discussion

In the present experimentation the flat coils exhibit the maximum energy efficiency of between 7 MHz to 8 MHz, if the values in Table 3 are taken, the resulting capacitor per coil to reach these resonant frequencies is listed in Table 5.

Table 5. Calculated parameters for the resonance frequency obtained in the experimentation.

Geometry	L (μH)	R (Ω)	C (pF)	Frequency
Square	3.39	1.4	152	7 MHz
Circular	2.84	1.0	139	8 MHz
Octagonal	2.76	1.0	143	8 MHz
Hexagonal	2.72	1.1	145	8 MHz

The capacitance of BNC connectors was evaluated with a UT8805E SERIES multimeter (UNI-T, n.d.), from which the device yielded a capacitance of 138 pF for each wire, with the data we can determine the parasitic capacitor of the coupled coils and their resonance frequency, the results are shown in Table 6.

Table 6. Parasitic capacitance for each proposed coil

Geometry	Coil C (pF)	Resonant freq.
Square	14	23.1 MHz
Circular	1	86 MHz
Octagonal	5	38.65 MHz
Hexagonal	7	32.67 MHz

To find the best geometry for flat coils, it is necessary to consider different factors to improve energy transmission. In the experiment, it was found that hexagonal coils transmit a higher inductive voltage compared to other coils at a 5 mm clearance. Another important factor is the number of turns. Xu Liu et al. (2016) in their experimentation with circular flat coils has shown the number of turns in the wired antenna determine the transmission efficiency of flat coils, therefore, it is necessary to develop more trials, but only in hexagonal coils at different numbers of turns to find the determined number of turns needed to establish the highest energy efficiency of inductive links.

Another interesting consideration was the high level of voltage detected in the receiving coil. This level was caused by the high impedance in the coils, as it behaved like an open circuit. Even at certain distances from the coil, a sufficient current was reached to ignite one LED with the mentioned frequency (see figure 11); in other cases, it was not so; therefore, even if the voltage is too high, it does not mean a high power, but rather a current transformation at a higher electrical potential in the receiving inductor compared to the transmitter.

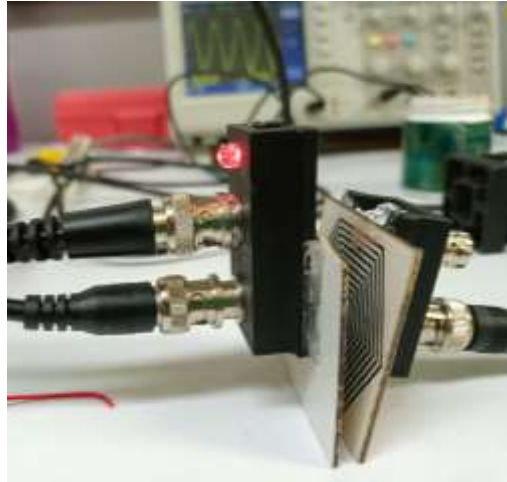


Fig. 11. Coil desalination current test with a light emitting diode

In the tests carried out, an attempt was made to obtain the current of the receiving coil to find its efficiency, however, the measurements obtained were different if only the voltage was recorded, this was largely due to the noise caused by the measuring instruments, for this reason was only limited to obtaining the voltage of the coils and therefore, the mutual inductance of the inductive link could not be obtained to be compared with the equations of raid and abbas (Abbas, Hannan, Samad, & Hussain, 2014), however, with this parameter the voltage was found higher at a certain frequency and particular geometry. Another study intended to record how the voltage varies at different inclinations and distances, using the frequency and geometry proposed in this work.

Acknowledgment

The authors of this project would thank the National Council of Humanities, Science and Technology (CONAHCYT-Mexico) for its partial support through the postdoctoral fellowship 490214 and the LANAVEX project 316256.

References

- ABB Robotics. (2021). *IRB-120 "Product specifications"* (3HAC035960-005). <https://library.e.abb.com/public/aeb809bf2b2a40208ca0719712b988b1/3HAC035960%20PS%20IRB%20120-es.pdf>
- Abbas, S. M., Hannan, M. A., Samad, S. A., & Hussain, A. (2014). Inductive coupling links for lowest misalignment effects in transcutaneous implanted devices. *Biomed Tech (Berl)*, 59(3), 257-268. <https://doi.org/10.1515/bmt-2013-0058>. PMID: 24445231.
- Alonso, M., Finn, E. J., Heras, C. A., & Barreto Araujo, J. A. (1970). *Física, Vol. II, Campos y Ondas*. Fondo Educativo Interamericano, S.A.
- Bosshard, R., Mühlethaler, J., Kolar, J. W., & Stevanović, I. (2013). Optimized magnetic design for inductive power transfer coils. In *2013 Twenty-Eighth Annual IEEE Applied Power Electronics Conference and Exposition (APEC)* (pp. 1812-1819). IEEE.
- Bouanou, T., El Fadil, H., Lassioui, A., Assaddiki, O., & Njili, S. (2021). Analysis of coil parameters and comparison of circular, rectangular, and hexagonal coils used in WPT system for electric vehicle charging. *World Electric Vehicle Journal*, 12(1), 45.
- Boylestad, R. L. (2017). *Introducción al análisis de circuitos* (13th ed.). Pearson.
- Chatterjee, S., Iyer, A., Bharatiraja, C., Vaghasia, I., & Rajesh, V. (2017). Design optimisation for an efficient wireless power transfer system for electric vehicles. *Energy Procedia*, 117, 1015-1023.

- Chen, W., Liu, C., Lee, C. H., & Shan, Z. (2016). Cost-effectiveness comparison of coupler designs of wireless power transfer for electric vehicle dynamic charging. *Energies*, 9(11), 906. <https://doi.org/10.3390/en9110906>
- Fang, Y., Hou, W., Zhou, W., & Zhang, H. (2018). Advances in implantable medical device battery. *Zhongguo Yi Liao Qi Xie Za Zhi*, 42(4), 272-275. <https://doi.org/10.3969/j.issn.1671-7104.2018.04.012>
- Harrison, R. R. (2007). Designing efficient inductive power links for implantable devices. In *2007 IEEE International Symposium on Circuits and Systems* (pp. 2080-2083). <https://doi.org/10.1109/ISCAS.2007.378508>
- Hernández Sebastián, N., Villa Villaseñor, N., Renero-Carrillo, F. J., Díaz Alonso, D., & Calleja Arriaga, W. (2020). Design of a fully integrated inductive coupling system: A discrete approach towards sensing ventricular pressure. *Sensors*, 20(5), 1525. <https://doi.org/10.3390/s20051525>
- Hernández, S. N. (2020). Desarrollo de un sensor de presión inalámbrico implantable para el monitoreo continuo de la presión ventricular [Doctor en ciencias en la especialidad de electrónica, Instituto Nacional de Astrofísica, Óptica y Electrónica]. Repositorio de tesis del Instituto Nacional de Astrofísica, Óptica y Electrónica. <https://inaoe.repositorioinstitucional.mx/jspui/bitstream/1009/1959/1/HernandezSeN.pdf>
- Hernández-Sebastián, N., Renero-Carrillo, F. J., Díaz-Alonso, D., & Calleja-Arriaga, W. (2019). Integrated bidirectional inductive-array design for power transfer in implantable BioMEMS. *Multidisciplinary Digital Publishing Institute Proceedings*, 15(1), 10.
- Liu, X., Xia, C., & Yuan, X. (2018). Study of the circular flat spiral coil structure effect on wireless power transfer system performance. *Energies*, 11, 2875. <https://doi.org/10.3390/en1112875>
- Montoya, T., Free, J., Gunderson, J., & Preheim, J. (n.d.). Tektronix TDS 2012, Digital Storage Oscilloscope. Retrieved from http://montoya.sdsmt.edu/ee220/handouts/tds2012_oscilloscope_guide.pdf
- Mutashar, S., Hannan, M. A., Samad, S. A., & Hussain, A. (2014). Analysis and optimization of spiral circular inductive coupling link for bio-implanted applications on air and within human tissue. *Sensors*, 14(7), 11522-11541. <https://doi.org/10.3390/s140711522>
- Ongayo, D., & Hanif, M. (2015). Comparison of circular and rectangular coil transformer parameters for wireless power transfer based on finite element analysis. In *2015 IEEE 13th Brazilian Power Electronics Conference and 1st Southern Power Electronics Conference (COBEP/SPEC)* (pp. 1-6). IEEE.
- Raise 3D. (n.d.). Pro2 3D Printer. Retrieved from <https://www.raise3d.com/products/pro2-3d-printer/>
- Rendon-Nava, A. E., Díaz-Méndez, J. A., Nino-de-Rivera, L., Calleja-Arriaga, W., Gil-Carrasco, F., & Díaz-Alonso, D. (2014). Study of the effect of distance and misalignment between magnetically coupled coils for wireless power transfer in intraocular pressure measurement. *The Scientific World Journal*, 2014. <https://doi.org/10.1155/2014/971586>
- Santiago-Amaya, J., López-García, C., Aguilar-Guggembuhl, J., & Sánchez-Díaz, F. X. (2022). Proposed algorithm for the design of planar inductors in implantable biomedical devices. *Journal of Technology and Innovation*, 9(25), 1-7. <https://doi.org/10.35429/JTI.2022.25.9.1.7>
- Shi, X., Qi, C., Qu, M., Ye, S., Wang, G., Sun, L., & Yu, Z. (2014). Effects of coil shapes on wireless power transfer via magnetic resonance coupling. *Journal of Electromagnetic Waves and Applications*, 28(11), 1316-1324. <https://doi.org/10.1080/09205071.2014.934999>
- UNI-T. (2021). UTG900E Series Function Arbitrary Waveform Generators. Retrieved from <https://instruments.uni-trend.com/static/upload/file/20210609/UTG900.pdf>
- UNI-T. (n.d.). UT81A/B Operating Manual, Scope Digital Multimeter. Retrieved from <https://meters.uni-trend.com/product/ut81-series/#Specifications>

UNI-T. (n.d.). UT8805E SERIES, Digital multimeter with 199999 counts. Retrieved from <https://instruments.uni-trend.com/multimeters/987.html>

Yang, Y., Cui, J., & Cui, X. (2020). Design and analysis of magnetic coils for optimizing the coupling coefficient in an electric vehicle wireless power transfer system. *Energies*, 13(16), 4143. <https://doi.org/10.3390/en13164143>

Zhao, J. (2010). A new calculation for designing multilayer planar spiral inductors. Retrieved from <https://www.edn.com/a-new-calculation-for-designing-multilayer-planar-spiral-inductors/>